Mechanical Properties and Fracture Patterns in Oil Palm Shell Concrete with Various Cement Types Using Digital Image Correlation

Handika, Nuraziz
Department of Civil Engineering, Faculty of Engineering, Universitas Indonesia

Bastian Okto Bangkit Sentosa
Department of Civil Engineering, Faculty of Engineering, Universitas Indonesia

Astutiningsih, Sotya
Department of Metallurgy and Material, Faculty of Engineering, Universitas Indonesia

Agung Gita Manohara
Department of Civil Engineering, Faculty of Engineering, Universitas Indonesia

他

https://doi.org/10.5109/7183449

出版情報：Evergreen. 11 (2), pp.1375-1382, 2024-06. 九州大学グリーンテクノロジー研究教育センター
バージョン：

Mechanical Properties and Fracture Patterns in Oil Palm Shell Concrete with Various Cement Types Using Digital Image Correlation

Nuraziz Handika[1,*], Bastian Okto Bangkit Sentosa[1], Sotya Astutiningsih[2], Agung Gita Manohara[1], Cellen Syafira Putri[1], Dini Rahmadhanti[1]

[1]Department of Civil Engineering, Faculty of Engineering, Universitas Indonesia, Indonesia

[2]Department of Metallurgy and Material, Faculty of Engineering, Universitas Indonesia, Indonesia

*Author to whom correspondence should be addressed:
E-mail: n.handika@ui.ac.id

(Received October 22, 2023; Revised March 5, 2024; Accepted April 30, 2024).

Abstract: Oil Palm Shell (OPS) aggregate has emerged as an applicable alternative construction material, with promising developments observed in the Structural and Material Laboratory. Previous research has demonstrated encouraging results with the utilization of OPS and Portland Composite Cement (PCC). This study aims to compare the mechanical characteristics of concrete with OPS aggregate using three types of cement: Ordinary Portland Cement (OPC), Portland Pozzolan Cement (PPC), and PCC. Various tests were conducted, including concrete compressive strength tests using cubical and cylindrical samples, tensile strength tests through Brazilian splitting tests, and flexural tests. Particularly, Digital Image Correlation (DIC) technique was employed during the compressive strength test to monitor specimen meticulously. These tests utilized standardized in terms of specimen size and mix design, differing only in the cement type used. The results revealed that OPC cement exhibited superior mechanical characteristics and structural performance compared to PPC and PCC cement. The average compressive strength of OPC-based concrete achieved 214 kg/cm², approximately equivalent to 20 MPa. These findings emphasize the potential of OPS aggregate in combination with OPC cement as a viable option for constructing robust and reliable buildings.

Keywords: Oil Palm Shell (OPS), OPS Concrete, Digital Image Correlation (DIC), Ordinary Portland Cement (OPC), Portland Pozzolan Cement (PPC), Portland Composite Cement (PCC)

1. Introduction

As the most widely used building material, concrete has witnessed a surge in demand for construction, necessitating the exploration of various alternative materials to substitute its components, either fine[1)], coarse aggregate, or the binder material. By product materials, including nickel slag[2)], various type of plastics[3)], polypropylene[4–6)], recycled aggregate[7)], fly ash[8)], hydro-removal ash[9)], and by-products of the palm oil industry[10)], have been investigated for this purpose.

Indonesia, as one of the largest producers of crude palm oil globally, generates around 85-90% of the total global palm oil production[11,12)]. Globally, massive production of this industry has led to the use of by-products from oil palm shell industries, not only in ethanol production[13)], heavy metal removal[14)] and energy[15)], but also in the domain of construction building materials[10,16–18)]. Oil palm shell (OPS), a by-product of the palm oil industry, has been identified as a viable, environmentally friendly alternative to coarse aggregates[10)] and as an additive[19)]. This development addresses the increasingly critical issues of solid waste management[20,21)], highlighting the potential of OPS in contributing to more sustainable construction practices.

Aligned with the Sustainable Development Goals (SDGs) Number 9 and 12, which emphasize the incorporation of innovative materials in construction and responsible resource utilization and waste management, the use of OPS in concrete represents a significant step in not only reducing the exploitation of natural aggregates and managing solid waste, but also contributing to the promotion of a circular economy[22)].

Previous research has shown promising outcomes when OPS is utilized in conjunction with Portland Composite Cement (PCC)[23–27)]. The research has covered various aspects, including the pre-treatment to prepare the OPS itself[27)], material characteristic tests[10,27)], its application in structural elements like simple beams[23,28)] and simple panels[24)], numerical simulations to study the damage resulting from compressive test using the damage model[25)] and even lifecycle assessments for simple structure in

laboratory application[29].

In the context of reducing CO_2 emissions, this study examines three types of cement, namely Ordinary Portland Cement (OPC), Portland Pozzolan Cement (PPC), and PCC. Each of these types has distinct compositions and characteristics that significantly impact the environment[30]. OPC primarily consists of clinkers, produced by heating limestone and other materials at high temperatures. It typically contains a high percentage of calcium silicates, calcium aluminates, and calcium aluminoferrites and contributing significantly to global CO_2 emission[31,32]. In contrast, PPC combines clinker with pozzolanic materials, such as fly ash or volcanic ash, which enhance the cement's properties and performance. Generally, PPC contains a lower percentage of clinkers compared to OPC. Similarly, PCC is a blend of clinker and supplementary cementitious materials like fly ash, slag, silica fume, or other pozzolanic materials. Similar to PPC, PCC also contains a lower percentage of clinkers resulting in reduced CO_2 emissions[33,34].

Modern technology has improved the precision of measurement in laboratory experimental activities. A technique called Digital Image Correlation (DIC) has been developed at the Laboratory of Structural and Material, Faculty of Engineering, Universitas Indonesia. DIC offers an advanced and non-contact approach to measure and analyze displacements, deformations, and strains in test specimens during the testing process. By employing digital image analysis, the DIC system tracks and compares each photo taken with the previous one, thereby capturing the motion changes the observed point[35,36]. It has been extensively used as an approach to study the mechanical properties of concrete, including deformation, modulus of elasticity and Poisson's ratio[2,37,38].

This research aims to further examine the mechanical properties of concrete containing OPS aggregate using OPC, PPC, and PCC. The OPS material was obtained from a distributor in the Greater Jakarta Area (*Jabodetabek*). The experimental research focuses on observing the mechanical response of OPS concrete through three characteristic tests: compressive strength tests using cubical and cylindrical samples, tensile strength tests using Brazilian splitting tests, and flexural tests. Digital Image Correlation (DIC) was employed specifically in the compressive strength test to monitor the movement of the specimen and subsequently analyze the deformation and fracture pattern of the cubical sample. In this research, the objective is also to examine any potential results from DIC.

Comparatively, the use of PPC and PCC shows different characteristics when interacting with OPS, in contrast to OPC, which is a pure Portland cement. The findings highlight that OPC cement exhibited excellent mechanical characteristics and structural performance compared to PPC and PCC cement, with an average compressive strength of 214 kg/cm², approximately equivalent to 20 MPa. These findings emphasize the potential of OPS aggregate in combination with OPC cement as a viable option for constructing robust and reliable buildings.

2. Materials and Methods

This section discusses the materials used in this research, including three types of cement, along with the material properties of sand and OPS.

2.1 Material of Oil Palm Shell Concrete

Material testing of fine aggregate (sand) and oil palm shell (OPS) was carried out in accordance with the SNI 03-2461-2002 standard for lightweight coarse aggregate. The OPS material, obtained from a distributor in the Greater Jakarta Area, comprises a mixture from various sub-species and regions in Indonesia, rather than being specifically sourced from a single province or plantation area. Notably, the OPS materials were stacked without any specific protective measures. The properties of OPS and sand are shown in Table 1, while Table 2 presents the Mix Design. Three types of cement were utilized. The OPS materials were pre-treated before the mixing process following previous research[27].

Table 1. Material Properties of OPS and Sand.

Material Properties	Oil palm shell (OPS)	Sand
Specific Gravity (SG)	1.340	2.625
Absorption	16.80%	0.40%
Bulk Density (Compacted)	594.37 kg/m³	1661 kg/m³
Size Max. Aggregate	12.50 mm	2.36 mm
Fineness Modulus (fm)	2.45	2.312
Abrasion Value	12.94%	-
Organic Content Test	No.5	No.4

Table 2. Mix Design Proportions.

Material Properties	Oil palm shell (OPS)
w/c	7/20
Cement (OPC, PCC, and PPC)	500
OPS	4.75-12. mm (273.4 kg/m^3)
Sand	0-5 mm (860 kg/m^3)

2.2 Concrete Characteristics Tests

The concrete characteristics tests conducted in this research included evaluations of compressive strength, split tensile strength, and flexural strength. These tests were performed in the laboratory, adhering to the established standards of SNI (Indonesia National Standard) and ASTM. Apart from comparing the characteristics of OPS concrete with OPC, PCC, and PPC cement mixtures, this testing aimed to establish correlations between each concrete property.

Compressive strength is defined as the maximum load per unit area that a test specimen can withstand before

failure under a specific compressive force applied by a testing machine. Cube compressive strength testing was performed on 28-day-old concrete samples measuring 15×15×15 cm^3, with a total of five samples. The cubes were removed from the curing tank two days before the testing but kept in high humidity condition to ensure a dry surface. Subsequently, the specimens were placed in the testing machine and subjected to a constant rate ranging from 2 to 4 kg/cm^2 per second until the point of failure.

According to SNI 03-2491-2002 standard, the split tensile strength test is designed to evaluate the tensile strength and shear resistance of lightweight concrete. The testing was performed using cylindrical samples with dimensions of D15×30 cm. The samples were positioned horizontally on the testing machine, and a constant loading rate of 0.7-14 MPa per minute was applied until the point of failure.

Flexural strength testing was conducted following the SNI 4431:2011 standard. The specimens measured 15×15×60 cm^3 and were placed exactly at the midpoint between two supports. The loading was applied at two points, spaced at one-third of the span length apart, making it a four-point loading simple beam test.

2.3 Digital Image Correlation (DIC)

During the compressive strength test, specifically cubical sample, a Fujifilm XA-3 camera was employed to conduct the Digital Image Correlation (DIC) test. However, the DIC system was not employed for the cylindrical compressive strength tests. The curved surface of the cylindrical samples poses challenges for tracking in the post-processing step with the current DIC methods developed in the laboratory. A digital camera was positioned in front of the sample to ensure that the entire sample was within the frame of the camera. Synchronization between the compressive test machine and the DIC system was maintained in terms of loading force application and timing to ensure precise post-processing analysis and reliable results.

The camera was configured to capture grayscale images in burst mode with a frame rate of 3 frames per second (fps). As pressure was applied to the samples, the camera recorded the movement of the speckle pattern on the surface of the concrete. This image capture process continued throughout the duration of the tests, allowing the camera to capture three pictures per second, facilitating better analysis and enabling the tracking of sample movement under compression loading.

The camera captured images of the specimen along with a stopwatch to synchronize the pictures with the applied load. The DIC testing was conducted solely on 28-day-old specimens. Figure 1 (a) shows the schema of DIC application in the laboratory. Figure 1 (b) illustrates the speckle pattern applied to the specimens before conducting the compressive test and DIC analysis. The speckle pattern was applied randomly in size, distance, and quantity using a permanent marker to ensure clarity and to prevent fading. This pattern aided the software in the post-processing to be tracked and to distinguish different parts of the specimen's surface.

Ensuring the camera's alignment with the specimen and the ground was critical for accurate DIC measurements, achieved by using a tripod to maintain uniformity and stability during image capture. Since the DIC system relies on the movement of the speckle pattern, it is essential to minimize any form of vibration that could affect the movement of camera during tests, including the use of camera remote shutter to capture pictures. Two lighting sources were utilized to assist in this process, maximizing the contrast between the speckle pattern and the white background of the sample.

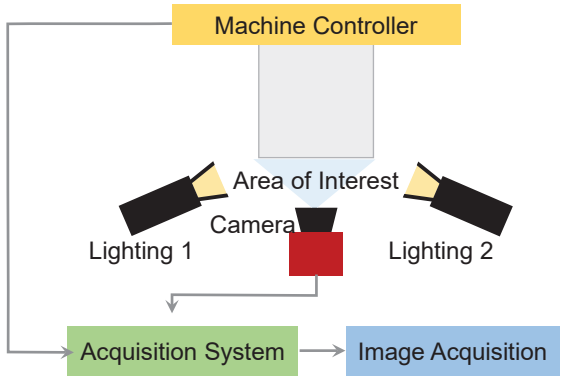

(a) Sketch of DIC system set up.

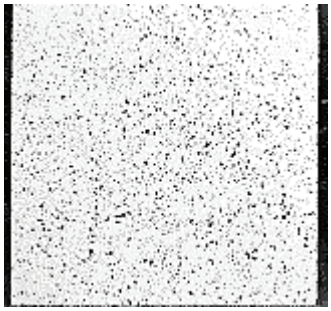

(b) Speckle pattern on specimen.

(c) DIC system set up in laboratory.

Fig. 1: Digital Image Correlation Set-Up.

3. Results and Discussions

3.1 Characteristics of OPS Concrete

Based on the results of the concrete characteristic tests, OPC cement exhibited the most dominant strength compared to the other two types of cement. This is evident

from previous research[38], which shows that OPC cement contains a high amount of calcium (Ca), resulting in the formation of Calcium Oxide (CaO), a crucial compound in cement hydration reactions. This high calcium content enables rapid reactions when Portland cement meets water, providing a significant increase in strength.

When comparing the results (as shown in Figs. 2, 3 and 4) with previous studies[23,24,27], the use of all three cement types in this research still resulted in lower strength. This discrepancy could be attributed to the use of different types of oil palm shells. This research used the mixed Oil Palm Shell (OPS) that was stocked in the Greater Jakarta Area. This condition was specifically conducted to understand the effects of using OPS with mixed sub-species and origin. Certain sub-species of palm oil have thick and bulky shells, whereas others have thin shells. Inconsistent particle sizes of the shells may lead to suboptimal strength outcomes.

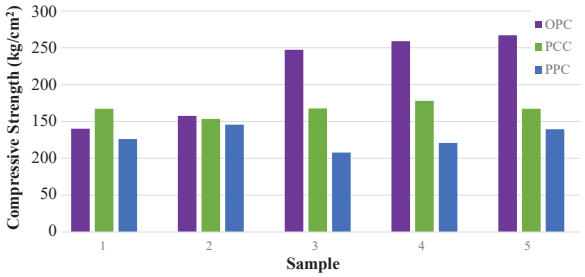

Fig. 2: Compressive strength results of OPS concrete (Cubical Samples).

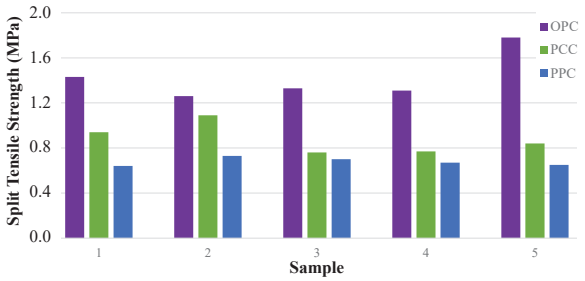

Fig. 3: Split tensile strength results of OPS concrete (Cylindrical Samples).

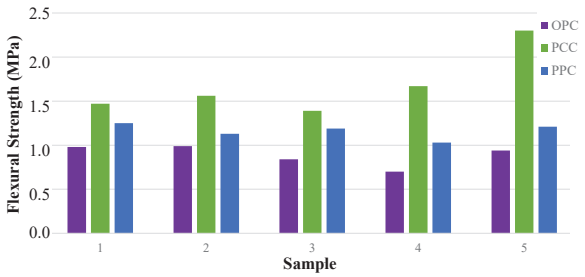

Fig. 4: Flexural strength results of OPS concrete (Beam Samples).

Consequently, only OPC cement met the minimum compressive strength requirements based on SNI 03-2461-2002 for structural lightweight concrete, which is 17 MPa (see Fig.2). Based on these results, the selection of certain sub-species is very important. The thickness of the OPS is important for the strength of the concrete. Previous research[23,24,27] used specific sub-species of palm shell from Bengkulu and Jambi.

Regarding Fig. 3, the same trend goes to split tensile strength of concrete. The splitting tensile strength results are approximately 8% for OPC, 6.36% for PPC, and 6.39% for PCC relative to compressive strength. The results are confirmed by the previous study that splitting tensile strength is 6.7%-8.1% of the compressive strength[39].

On the other hand, the flexural strength of OPC OPS concrete was not as good as the split tensile strength and compressive strength, see Fig. 4. OPC cement exhibited a different behavior, with the lowest flexural strength values compared to the other two cement types. Using PCC type of cement results in better flexural strength. The flexural strength results are higher than the splitting tensile strength. These are approximately 12.13% for PPC, and 10.95% for PCC relative to compressive strength. This condition is largely influenced by moisture content of OPC and difference physical strength of the coarse aggregate. It is also possible that the problem comes from the storage of OPC cement in the laboratory.

3.2 Load-Displacement Response from DIC

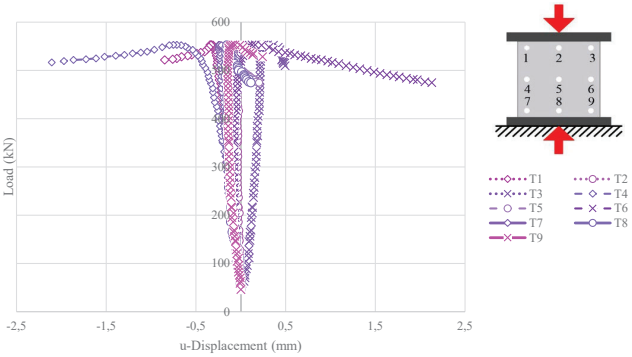

Fig. 5: Experimental results: Load-*u* displacement response of OPS with OPC concrete (Cube Samples).

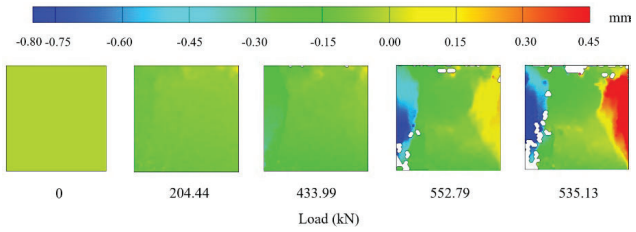

Fig. 6: Experimental results: *u*-displacement field of OPS with OPC concrete (Cube Samples).

The force-displacement relationship in the *x*-direction (*u*-displacement) for OPS with OPC concrete is presented in Fig. 5, while the displacement field in the *x*-direction steps are shown in Fig. 6.

Based on the graphs depicting the horizontal displacements, the displacements at nine observation points exhibit a linear behavior during the linear elastic phase. In this phase, the concrete demonstrates an elastic

response to the applied load, where it can return to its original state without experiencing permanent deformation. However, the displacements become nonlinear when the fracture starts to appear, signifying the transition from the elastic phase to the semi-plastic phase. Upon reaching the maximum load condition, the concrete enters the plastic phase, indicating larger displacements compared to the elastic phase, and resulting in permanent deformations. During this phase, as the concrete reaches its elastic limit, continuous plastic deformations occur with increasing loads.

When the concrete reaches its maximum strength, and its load-carrying capacity is exceeded, fractures begin to form and propagate along the surface. This indicates that the concrete has entered the failure phase, characterized by a decline in its strength upon loading. Fig. 5 illustrates that the displacements tend to move towards the right and to the left of the *x*-axis of the specimen, identifying the locations of movement of the specimen in *x*-direction. Point number 1, 4 and 7 move to the left according to the receive loading application. Fig. 6 confirms the movement of the points. The left side of the cube specimen moves to the left as the fractures open. Meanwhile, point 3, 6 and 9 show the opposite condition, movement to the right (see the red color area in Fig. 6).

Displacement in *x*-direction describes the horizontal displacement of the cube in response to the applied loading. This initial verification of the sample's response is critical for verifying the suitability of DIC for further analysis. It helps in controlling the eccentricity of the load relative to the concrete cubes. Examination of the detailed movements at points 4 and 6, see Figs. 5 and 6, reveals a symmetrical response to the loading: point 4 displaces leftward, while point 6 shifts rightward, aligning with the anticipated behavior. Such observations also confirm the uniform distribution of OPS aggregates within the sample. Moreover, post-processing analysis of DIC system effectively captures these conditions, marking the reliability and accuracy of this measurement technique.

The force-displacement responses in the *y*-direction (*v*-displacement) of OPS with OPC concrete are illustrated in Fig. 7, while the displacement field in the *y*-direction (*v*-displacement) are shown in Fig. 8. Same as previously mentioned in *x*-direction, from the force-displacement curve in *y*-direction, at the beginning the concrete behaves linearly elastic. Gradually, the concrete's mechanical properties transform from semi-plastic to plastic upon reaching and surpassing the maximum load.

In this phase, the concrete experiences larger displacements compared to when it was in the elastic phase, with deformations continuing and becoming permanent until the concrete reaches its maximum strength and load-bearing capacity is exceeded. This is evidenced by the propagation of cracks along the concrete surface, signifying the onset of the failure phase, accompanied by a decline in concrete strength upon loading.

Fig. 8 confirms the movement of the nine points. Due to the applied loading, fractures occur, and the movement direction of point one is downward. In the curve in Fig. 7, the point is in negative value. The opposite condition occurs in point 8. From Fig. 5 to 8, it can be said that the DIC system catches the realistic movement of each point.

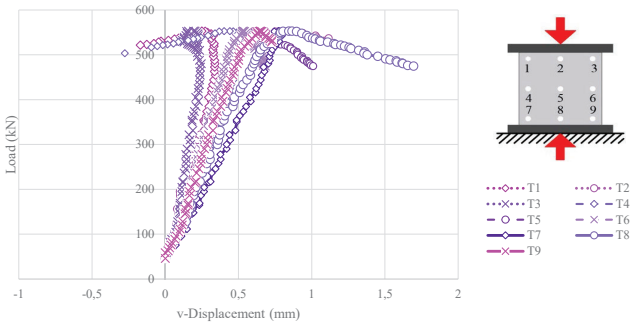

Fig. 7: Experimental results: Load-*v* displacement response of OPS with OPC concrete (Cube Samples).

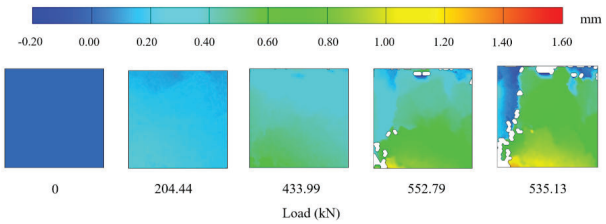

Fig. 8: Experimental results: *v*-displacement field of OPS with OPC concrete (Cube Samples).

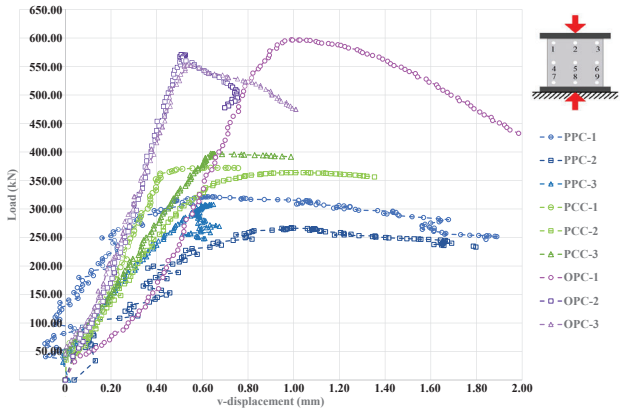

Fig. 9: Experimental results: Load- v displacement response of OPS with OPC, PPC, and PCC concrete (Cube Samples).

The load-displacement graph presented in Fig. 9 depicts points representing the displacements occurring in each test specimen. It can be observed that each sample, including OPS concrete with OPC, PPC, and PCC, exhibits different deformations at each loading phase. From the graph, it is evident that not all samples enter the linear elastic phase during the initial loading, indicating that the initial displacements are not solely due to the elastic response of the concrete. This non-linear behavior can be attributed to the low homogeneity of the concrete, resulting in uneven load distribution when the load is

applied. All curves in Fig. 9 represent the average movement of 9 points for each sample. The peak of the force-displacement curve for OPC OPS concrete, marking highest values, serves as evidence of the behavior shown in the curves in Fig. 2.

3.3 Fracture Patterns

The results of the major strain diagrams for OPS concrete with OPC, PCC, and PPC cement are presented in Fig. 10. Major strain was selected to illustrate crack opening, and the diagram shows the evolution of fractures at each load increment. According to BS EN 12390-3-2009 - Testing Hardened Concrete, the crack/ fracture patterns observed in the OPC, PCC, and PPC samples are categorized as satisfactory failures, where cracks occur uniformly on the surface of the specimens.

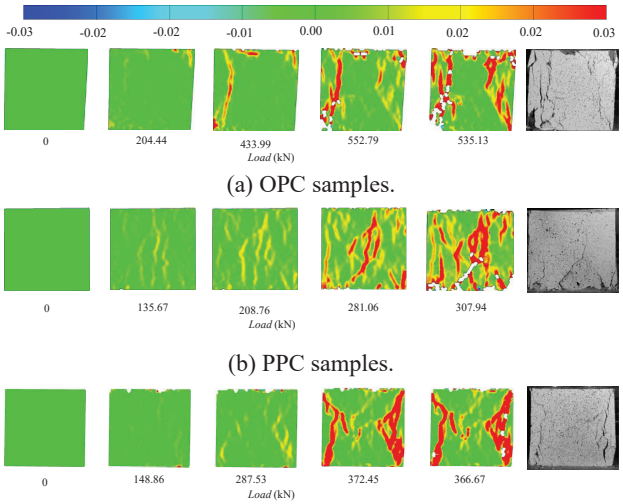

(a) OPC samples.

(b) PPC samples.

(C) PCC samples.

Fig. 10: Experimental results: major strain field of OPS with OPC, PCC and PPC concrete (Cube Samples).

Figures 11(b) and (c) display the fracture patterns for OPS concrete with OPC categorized as satisfactory failures, with fracture/ cracks uniformly distributed over the entire surface of the cubes. However, Figure 11(a) exhibits an unsatisfactory failure pattern, where cracks are not evenly distributed. Figure 11(c) shows a PCC concrete sample with satisfactory failures, while Figs. 11(e) and (f) demonstrate unsatisfactory failures with dominant cracks occurring on one side of the sample. In the case of PPC concrete, crack patterns in Figs. 11(h) and (i) are categorized as satisfactory failures, while Fig. 11(g) shows unsatisfactory failures with unevenly distributed cracks.

The occurrence of unsatisfactory fracture/ crack patterns can be attributed to the improper positioning of the cubical specimen during test or the uneven distribution of aggregate inside the sample. In the case of improper positioning, inaccuracies in specimen placement on the testing machine led to uneven crack distribution across the cube. During the test, this condition was prevented, and proper placement was performed. Satisfactory failures in crack patterns were observed in OPC samples 2 and 3, PCC sample 1, as well as PPC samples 2 and 3, where cracks were uniformly distributed on all sides of the specimens. Unsatisfactory failures were observed in PPC samples 2 and 3, with cracks occurring on only one side. Thus, this condition may be due to uneven distribution of OPS aggregates within the sample. Furthermore, unsatisfactory failures were also observed in OPC sample 1 (Fig. 11(a)) and PPC sample 1 (Fig. 11(d)), with tensile cracks resulting from non-centrally positioned specimens.

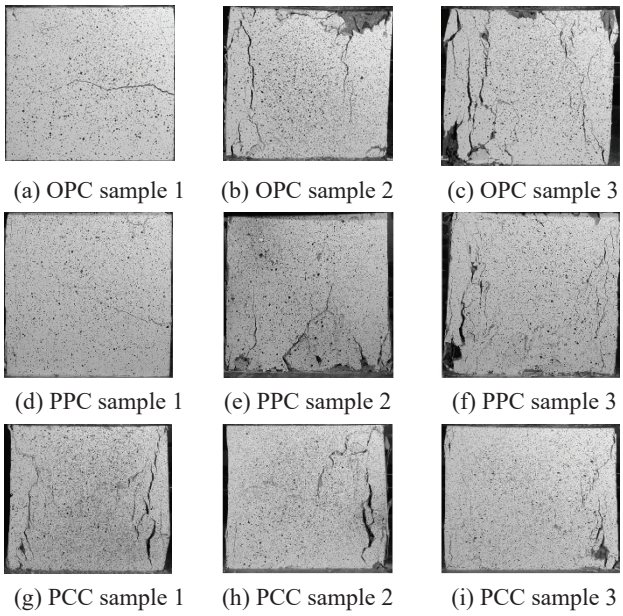

(a) OPC sample 1 (b) OPC sample 2 (c) OPC sample 3

(d) PPC sample 1 (e) PPC sample 2 (f) PPC sample 3

(g) PCC sample 1 (h) PCC sample 2 (i) PCC sample 3

Fig. 11: Experimental results: conditions of concrete sample at the end of the test for OPS with OPC, PCC and PPC cement (cube samples).

4. Conclusion and future recommendations

The use of mixed sub-species of oil palm shell generally results in lower concrete compressive strength. This proves that the selection of OPS sub-species significantly influences the strength of OPS concrete. Based on the laboratory experiments conducted in this research, OPS concrete with OPC cement exhibited higher compressive and tensile strength compared to OPS concrete with PPC and PCC cements. The average compressive strength achieved at 28 days was 214.05 kg/m³ or approximately 20 MPa, while the average tensile strength was 1.42 MPa. However, OPS concrete with OPC cement showed less favorable performance in flexural strength when compared to PPC and PCC mixes.

Due to their reduced clinker content and incorporation of supplementary materials, both PPC and PCC offer potential sustainability benefits compared to OPC. Regarding the study results, OPC OPS concrete is not recommended for application on rigid pavement as it is dominated with flexural strength. However, the choice of

the best cement type for a construction project should consider a holistic assessment of sustainability factors, including environmental impact and economic feasibility.

The Digital Image Correlation (DIC) system, utilizing the GOM Correlate software, was employed to generate load-displacement responses for samples using the three different types of cement. The vertical displacement-load relationship demonstrated the concrete's behavior from the initial stages. By examining displacements and strains in both the *x* and *y* directions, the early age of cracks and eventual concrete failure were detected, as captured in the final photos of each specimen. The DIC system proved to be an effective tool for analyzing the behavior and mechanical properties of materials, contributing to the development of safer and more efficient testing practices.

As displacement in *x* and *y*-direction are obtained from DIC, theoretically, modulus of elasticity and Poisson's ratio can be deducted as performed in previous research [2,37,38]. Nevertheless, it requires standardized tests to obtain these two properties. Thus, future work can be done by performing comparative experimental studies using standardized method and DIC system approach to obtain modulus of elasticity and Poisson's ratio.

Another future work, it is suggested to use selected sub-species of OPS aggregate to obtain better compressive concrete. Further study can be performed using OPC and OPS aggregate, such as permeability and testing for structural elements (simple beam and/or slab).

Acknowledgements

This study is funded by BPDPKS (*Badan Pengelola Dana Perkebunan Kelapa Sawit*) Research Grant 2021-2022.

References

1) Singh S., Singh S.K., Kumar R., Shrama A., and Kanga S., "Finding alternative to river sand in building construction | collections | kyushu university library," *Evergr. Jt. J. Nov. Carbon Resour. Sci. Green Asia Strategy*, 09 (*04*) 973–992 (2022). https://doi.org/10.5109/6625713
2) E. Ernawan, J. Sjah, N. Handika, S. Astutiningsih, and E. Vincens, "Mechanical properties of concrete containing ferronickel slag as fine aggregate substitute using digital image correlation analysis," *Buildings*, 13 (*6*) 1463 (2023). doi:10.3390/buildings13061463.
3) Y.-S. Lee, "Waste/recycled plastics in concrete," 7 103–110 (2019). doi:10.5281/zenodo.6014696.
4) H. Purnomo, M. Chalid, G. Pamudji, and T.W. Arrifian, "Bond–slip relationship between sand-coated polypropylene coarse aggregate concrete and plain rebar," *Materials*, 15 (*7*) 2643 (2022). doi:10.3390/ma15072643.
5) G. Pamudji, M. Satim, M. Chalid, and H. Purnomo, "The influence of river and volcanic sand as coatings on polypropylene waste coarse aggregate towards concrete compressive strength," *J. Teknol.*, 82 (*4*) (2020). doi:10.11113/jt.v82.14124.
6) J. Sjah, J. Chandra, J. Rastandi, and E. Arijoeni, "The effect of usage of crushed polypropylene plastic waste in mechanical properties of concrete," *Int. J. Civ. Eng. Technol.*, 9 1495–1505 (2018).
7) N. Handika, B.F. Norita, E. Tjahjono, and E. Arijoeni, "Experimental studies on the homogeneity and compressive strength prediction of recycled aggregate concrete (rac) using ultrasonic pulse velocity (upv)," (n.d.). doi:https://doi.org/10.32783/csid-jid.v3i2.111.
8) S.W.M. Supit and Priyono, "The Use of Fly Ash in Pervious Concrete Containing Plastic Waste Aggregate for Sustainable Green Infrastructure," in: H.A. Lie, M. Sutrisna, J. Prasetijo, B.H.W. Hadikusumo, L.S. Putranto (Eds.), Proc. Second Int. Conf. Constr. Infrastruct. Mater., Springer, Singapore, 2022: pp. 141–152. doi:10.1007/978-981-16-7949-0_13.
9) Zhakypova G., Uderbayev S., Saktaganova N., Abyieva G., Budikova A., and Zhapakhova N., "Properties of fine-grained concrete using ash of kazakhstan | collections | kyushu university library," *Evergr. Jt. J. Nov. Carbon Resour. Sci. Green Asia Strategy*, 10 (*02*) 830–841 (2023). https://doi.org/10.5109/6792835
10) E. Tjahjono, A.M. Fani, D.D. Dodi, E.P. Purnamasari, F.A. Silaban, and E. Arijoeni, "The study of oil palm shell (ops) lightweight concrete using superplasticizer, silica fume, and fly ash," *Mater. Sci. Forum*, (2017). doi:10.4028/www.scientific.net/MSF.902.65.
11) B.P.D.P.K.S. BPDPKS, "Enhancement of Palm Oil Plantation Productivity to Support Inclusive and Sustainable Palm Oil Transformation. Annual Report 2022 Badan Pengelola Dana Perkebunan Kelapa Sawit (Oil Palm Plantation Fund Management Agency)," n.d.
12) Directorate General of Plantations, "Directorate general of plantations. statistic of indonesia plantation: three crop estate statistics of indonesia 2015-2017 kelapa sawit palm oil (2016).," (2019).
13) Sahlan M., Muryanto, Hermansyah H., Wijanarko A., Gozan M., Lischer K., Ahmudi A., and Pujianto P., "Ethanol production by encapsulated rhizopus oryzae from oil palm empty fruit bunch | collections | kyushu university library," *Evergr. Jt. J. Nov. Carbon Resour. Sci. Green Asia Strategy*, 07 (*01*) 92–96 (2020). https://doi.org/10.5109/2740963
14) E. Khankhaje, T. Kim, H. Jang, C.-S. Kim, J. Kim, and M. Rafieizonooz, "Dataset on the assessment of pervious concrete containing palm oil kernel shell and seashell in heavy metal removal from stormwater," *Data Brief*, 50 109570 (2023). doi:10.1016/j.dib.2023.109570.
15) "Cost-effective synthesis of ceo_2-sio_2 based on oil palm leaves for the removal of toxic compounds | collections | kyushu university library," (n.d.). https://hdl.handle.net/2324/7151676 (accessed October 20, 2023).
16) U. Johnson Alengaram, M.Z. Jumaat, H. Mahmud, and M.M. Fayyadh, "Shear behaviour of reinforced palm kernel shell concrete beams," *Constr. Build.*

Mater., 25 (*6*) 2918–2927 (2011). doi:10.1016/j.conbuildmat.2010.12.032.
17) H. Hamada, F. Abed, A. Alattar, F. Yahaya, B. Tayeh, and Y.I.A. Aisheh, "Influence of palm oil fuel ash on the high strength and ultra-high performance concrete: a comprehensive review," *Eng. Sci. Technol. Int. J.*, 45 101492 (2023). doi:10.1016/j.jestch.2023.101492.
18) S.N. Chinnu, S.N. Minnu, A. Bahurudeen, and R. Senthilkumar, "Influence of palm oil fuel ash in concrete and a systematic comparison with widely accepted fly ash and slag: a step towards sustainable reuse of agro-waste ashes," *Clean. Mater.*, 5 100122 (2022). doi:10.1016/j.clema.2022.100122.
19) B.H.S. Amartey, T.J. Kumator, Y.D. Amartey, and A. Ali, "The use of oil palm fibre as an additive in concrete," *Mater. Today Proc.*, 86 111–115 (2023). doi:10.1016/j.matpr.2023.03.820.
20) À. Maldonado-Alameda, J. Giro-Paloma, A. Alfocea-Roig, J. Formosa, and J.M. Chimenos, "Municipal solid waste incineration bottom ash as sole precursor in the alkali-activated binder formulation," *Appl. Sci.*, 10 (*12*) 4129 (2020). doi:10.3390/app10124129.
21) Zhumadilova A., and Zhigitova S., "Features of modern areas of solid waste disposal | collections | kyushu university library," *Evergr. Jt. J. Nov. Carbon Resour. Sci. Green Asia Strategy*, 10 (*02*) 640–648 (2023). https://doi.org/10.5109/6792809
22) Agarwal S., Tyagi M., and Garg R.K., "Circular economy reinforcement to diminish ghg emissions: a grey dematel approach | collections | kyushu university library," *Evergr. Jt. J. Nov. Carbon Resour. Sci. Green Asia Strategy*, 10 (*01*) 389–403 (2023). https://doi.org/10.5109/6781099
23) F.D. Sofyani, N. Handika, E. Tjahjono, and E. Arijoeni, "Flexural behaviour of reinforced lightweight concrete beam using hot water pre-treated oil palm shell coarse aggregate," *MATEC Web Conf.*, 276 01032 (2019). doi:10.1051/matecconf/201927601032.
24) A.M. Fani, N. Handika, E. Tjahjono, and E. Arijoeni, "Flexural behaviour of reinforced lightweight concrete floor panel using hot water pre-treated oil palm shell as coarse aggregate," *AIP Conf. Proc.*, 2114 (*1*) 040001 (2019). doi:10.1063/1.5112430.
25) K. Hongsen, M. Melhan, N. Handika, and B.O.B. Sentosa, "Parameterization of oil palm shell concrete on numerical damage model based on laboratory experiment using digital image correlation," *J. Phys. Conf. Ser.*, 1858 (*1*) 012029 (2021). doi:10.1088/1742-6596/1858/1/012029.
26) B.J. Parmadi, N. Handika, D. Sutanto, and B.O.B. Sentosa, "Recycled aggregate concrete beam: experimental study using digital image correlation (dic) and numerical study using multi-fibre timoshenko beam element in cast3m," *AIP Conf. Proc.*, 2847 (*1*) 050011 (2023). doi:10.1063/5.0179561.
27) S.T. Lee, N. Handika, E. Tjahjono, and E. Arijoeni, "Study on the effect of pre-treatment of oil palm shell (ops) as coarse aggregate using hot water 50-°c and room temperature water 28-°c to lightweight concrete strength," *MATEC Web Conf.*, 276 01023 (2019). doi:10.1051/matecconf/201927601023.
28) N. Handika, F. D Sofyani, E. Tjahjono, and E. Arijoeni, "Cracking behavior of reinforced lightweight concrete beam using hot water pre-treated oil palm shell coarse aggregate," *IOP Conf. Ser. Mater. Sci. Eng.*, 473 012030 (2019). doi:10.1088/1757-899X/473/1/012030.
29) D.A. Ospaman, N. Handika, and D. Wulandari, "Life cycle assessment of lightweight beam concrete made from oil palm shell coarse aggregate," (2022). https://easychair.org/publications/preprint/NJ6w (accessed August 4, 2022).
30) P.-C. Aïtcin, "4 - Supplementary cementitious materials and blended cements," in: P.-C. Aïtcin, R.J. Flatt (Eds.), Sci. Technol. Concr. Admix., Woodhead Publishing, 2016: pp. 53–73. doi:10.1016/B978-0-08-100693-1.00004-7.
31) Z. He, X. Zhu, J. Wang, M. Mu, and Y. Wang, "Comparison of co2 emissions from opc and recycled cement production," *Constr. Build. Mater.*, 211 965–973 (2019). doi:10.1016/j.conbuildmat.2019.03.289.
32) A. Naqi, and J.G. Jang, "Recent progress in green cement technology utilizing low-carbon emission fuels and raw materials: a review," *Sustainability*, 11 (*2*) 537 (2019). doi:10.3390/su11020537.
33) P.S. Darmanto, and A. Amalia, "Analysis of high clinker ratio of portland composite cement (pcc)," *South Afr. J. Chem. Eng.*, 34 116–126 (2020). doi:10.1016/j.sajce.2020.07.010.
34) V. Nari, P.H. Praneeth, and V. manchana, "A comparative study on the thermal behaviour of ppc and opc cement," *Mater. Today Proc.*, 39 1588–1593 (2021). doi:10.1016/j.matpr.2020.05.708.
35) M.A. Sutton, J.J. Orteu, and H. Schreier, "Image Correlation for Shape, Motion and Deformation Measurements: Basic Concepts,Theory and Applications," Springer US, 2009. doi:10.1007/978-0-387-78747-3.
36) J. Curt, M. Capaldo, F. Hild, and S. Roux, "Optimal digital color image correlation," *Opt. Lasers Eng.*, 127 105896 (2020). doi:10.1016/j.optlaseng.2019.105896.
37) A.D. Deltanto, N. Handika, and B.O.B. Sentosa, "Response of load-displacement on cubical sample of oil-palm shell with fly ash concrete using digital image correlation system," *AIP Conf. Proc.*, 2376 (*1*) 040007 (2021). doi:10.1063/5.0063958.
38) F.F. Rahman, W.A. Prakoso, E. Tjahjono, B.O.B. Sentosa, and M. Orientilize, "Load-displacement response of oil palm shell concrete compressive test using digital image correlation," *IOP Conf. Ser. Earth Environ. Sci.*, 498 012037 (2020). doi:10.1088/1755-1315/498/1/012037.
39) P. Shafigh, M.Z. Jumaat, H.B. Mahmud, and N.A.A. Hamid, "Lightweight concrete made from crushed oil palm shell: tensile strength and effect of initial curing on compressive strength," *Constr. Build. Mater.*, 27 (*1*) 252–258 (2012). doi:10.1016/j.conbuildmat.2011.07.051.